A Multi-Robot System Architecture for Trajectory Control of Groups of People

Edgar A. Martinez-Garcia, Akihisa Ohya & Shinichi Yuta

1. Introduction

How to conduct a group of humans towards a target destination by a team of robots is the key-problem discussed in the present context. A suitable multi-robot system (MRS) architecture has been investigated and implemented for guiding groups of people. The present system can be seen as guiding-tours, nevertheless further than such concept this implementation can be though, or it is closer to the model given by several dogs flocking herds of sheep, guiding them towards a targeted place. Dogs and sheep have a minimal way of explicit communication. Sheep herd's trajectory is controlled by a team of dogs (even one). The dogs do bark and/or approach to the herd if there is any situation disordering guidance. The proposed context differs from it, since does not exist any type of explicit signal for guidance, and trajectory control is given by a way based on natural reactions of angle-velocity motions between humans and robots. An extensive theoretical description and experimental results are discussed. Recent progress in robotics and artificial intelligence has made possible to build interactive mobile robots that operate highly reliably in crowded environments. There exist in the research field community several works concerned with guiding-tours, nevertheless tackling different problems and/or deploying different architectures. Few successful works concerned with guiding-tours have been developed (Nourbakhsh et al., 1999; Thrapp et al., 2001; Burgard et al., 1999). Our context has some differences, such as our system is compounded by a team of mobile robots, due to the importance of the task our architecture is centralized and deliberative, the MRS controls the people trajectory motion, and communication between robots and people is based on motion reactions. Section 2 discusses in the limits and scope of this research; section 3 details the architectural framework of the MRS. In section 4 a methodology for people localization by the MRS is presented in deeply. The section 5 briefly describes a proposed strategy for control of the conduction task, while in section 6 the part of robots motion planning is treated. Finally, section 7 and 8 shows simulation results of the proposed methodologies, and the conclusions respectively in each section.

2. Aim of Study

In the present context guided tours are defined as walking or moving from one point to a target location by performing certain conduction tasks, essentially involving mechanisms to crowd people. Three main issues have been regarded as part of the process of conduction:

Source: Cutting Edge Robotics, ISBN 3-86611-038-3, pp. 784, ARS/plV, Germany, July 2005 Edited by: Kordic, V.; Lazinica, A. & Merdan, M.

1.) Guiding is defined as the conduction of the group of people through the pathway, by the Ra easily followed by the group of humans (all conditions are kept in a normal status);
2.) Crowding (group size Control). It is the process of collecting the group together still closer than it actually is, while the group keeps striding on the pathway. So, in this context an undesirable situation is when the size of the group area (radius r_k) increases at discrete time k, such that becomes bigger than a desired size or radius r_{ref};
3.) Interception. Another situation is when a person intents to leave the group, or moving away from its scope. It is called interception, because a given robot approximates to he/she attempting to yield the person going back the group. However, despite this task has been considered, it leads to face other challenging problems, but for now it is out of the scope of this chapter.

2.1 Strategy for MRS-based Guidance

The main reason of configuration in Fig. 1 is because only one robot is needed as long as for guidance or conduction is concerned. On the other hand, two vehicles are settled at back-side to observe the people's behavior and/or crowd the group whether it is necessary by means of special guiding tasks.

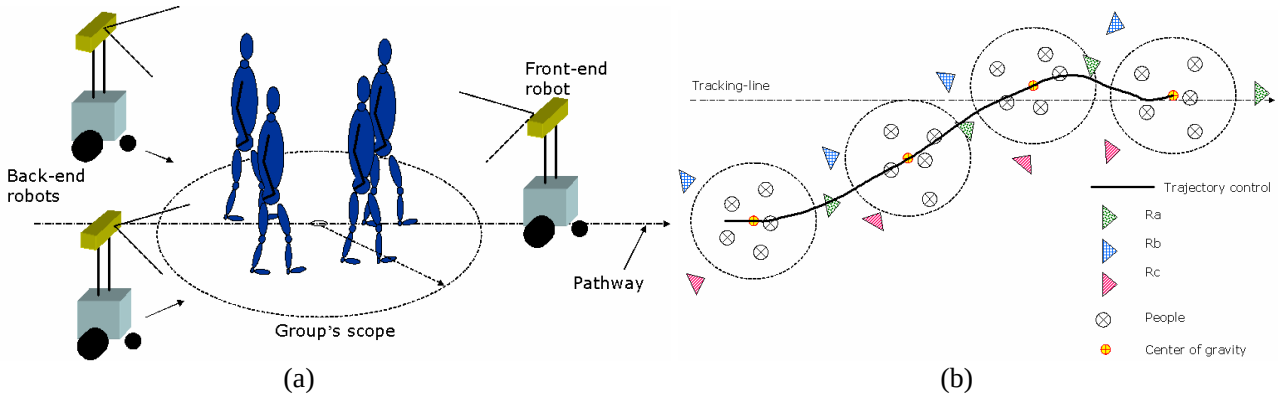

(a) (b)

Figure 1. (a) Robots' formation conducting a group of people; (b) The team of robots in formation steering the group of people's trajectory

In order to represent the area coverage of a group of people, we established a circular model which encompasses all the members together as depicted in Fig.1) and Fig.2. Until up now, we have restricted it with a number of people between 2 up to 6 persons in hallways of the University of Tsukuba. The CG is expressed by its components (x; z; θ, v, w), and the MRS senses a measure of it at location (x; z) and heading angle θ, with lineal displacement in XZ-space vk, and angular velocity wk at discrete time k. Thus, CG heading angle represents the group's direction towards it is being displaced or will be displaced.
The presented strategy was planned for accomplishing conduction and it can be divided as follows:
1) Stereo vision-based people tracking.
2) MRS architecture design.
3) People trajectory control and robots motion planning.

The item number 1 will be discussed in latter sections, but for further reference it also was presented by the authors in references (Martinez et al., 2003; Martinez-Garcia et al., 2004). The item 2 was presented in (Martinez-Garcia et al., 2005). And item 3 is roughly discussed in latter sections.

3. Multi-Robot System Architecture

The robots conducts the people by a non-active cooperative modality (Murphy, 2000), sharing sensor data, cooperating for tracking and conducting the people without knowing on the existence of other robots. The architecture is compounded by a central host and a team of 3 self-contained mobile robots mechanically homogeneous, although we may think of it, that they can be considered heterogeneous since at least one robot's differences (front-side) arise more functional rather than physical (depicted in Fig.3-(b)). Deliberation is performed in the central host that remains during the entire mission duration as similar architectur presented in (Iocchi et al., 1995) and described in (Cao et al., 1997). A first endeavor of this architecture is to share distributed sensory information. It was established that a reliable way to share distributed percepts was by (1) performing a separate filtering process in each robot; and (2) to carry out with multi-sensor data fusion in the central host as depicted in Fig.3-(a).

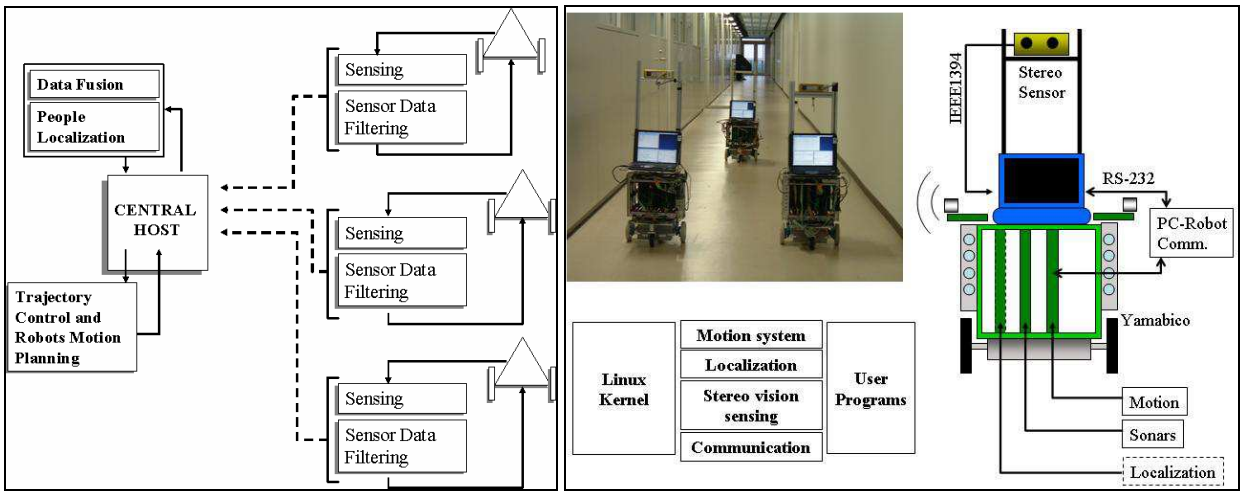

(a) (b)

Figure 2. (a) MRS architecture; (b) robots platform and configuration

The MRS exploits the stereo vision model; because stereo-based ranging data has several favorable points for world sensing in this context. It facilitates: (1) 3D spatial coordinates in real-time; (2) object segmentation (Beymer & Konolige, 1999), although, such advantages could be obtained by other methods and sensors. Each mobile robot was equipped with commercially available stereo vision sensors that provide disparity maps (sum of absolute differences), gray scale images (160x120 pixels) in real-time acquired by an IEEE 1394 bus communication. Each laptop on-board is 900MHz Pentium-III running under Linux. The Fig. 3-(a) depicts the configuration of the robots required for sensing a person (including gray level image and disparity map obtained from experiments). The disparity map represents a matching of the ranged environment by levels of gray. The farther a point is from the sensor, the more darken the pixel becomes. The center of the sensor was fitted approximately at 100cm height. In addition, the stereo parameters were established a priori by choosing and changing such settings manually until they met our

needs. In earlier experiments world was measured within an empty area of approximately 800x700cm with a human standing at 200cm away from the sensor for evaluating stereo parameters, sensor's accuracy, measuring timing and sensory info analysis. A first complication in using this model was high rate of noise due to stereo occlusion, and light conditions.
The experimental results are depicted in Fig. 3-(b) that shows the top and side views of sensor data plotting, robot's sensor at (0, 100, 0).

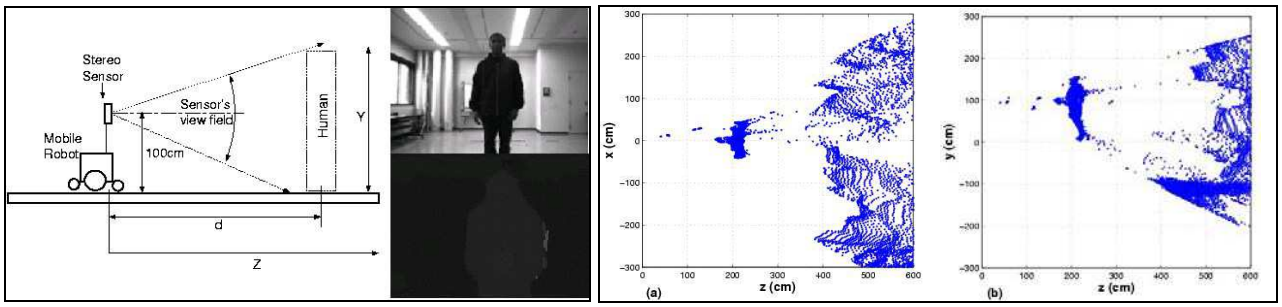

(a) (b)

Figure 3. (a) Robot configuration, gray level image and disparity map; (b) ranged data, top and side views

Furthermore, the multi-robot communication system is based on functions for spreading messages and a group-communication philosophy (Fig.4-(a)), as similar architecture presented in (Iocchi et al., 2003). Each laptop on-board has wireless technology via IEEE802.11b. Experimental results on the MRS trade-offs such as sensory info and robots pose sharing are shown in table 1, real needs include transferring messages of about 1kb, nevertheless transactions were performed with 100kb. See (Martinez-Garcia et al, 2005) for further details on the communication architecture. In addition, another issue that depends on the MRS communication architecture is during the guiding-task performance robots localization, which is a critical issue for the team of robots.

Experiments	Ra to the central-host	Rb to the central-host	Rc to the central-host
1	8	9	7
2	10	8	9

Table 1. Time (ms) spent in a round trip for 100 kbytes

Self-localization is accomplished in a cooperative framework, where robots do share a relative Common Cartesian Coordinate System (CCCS). The CCCS development and its usage were presented by the authors in (Martinez-Garcia et al., 2005; Yoshida et al., 2003). The CCCS facilitates the problem of robots localization by sharing a relative system among robots without any world map in advance. The CCCS is an architectural framework embedded in each robotic platform (Yoshida et al., 2003). The method is based on matching measurements arising from ultrasonic range sonar and odometers. The 3 mobile robots get their pose respect to the objects in the world; if there are differences, the robots self-correct such measurements. Nevertheless, since CCCS is unable to self-correct error pose in navigation time, only Ra deploys a special pose estimator system (Watanabe & Yuta, 1990) aimed to correct positional errors. Measurements arising from CCCS and the pose estimator are combined into the central host, which have a global model of the world to overcome the problem of localization and navigation of the robots. The sequence of steps for such process is described in Fig.4-(b).

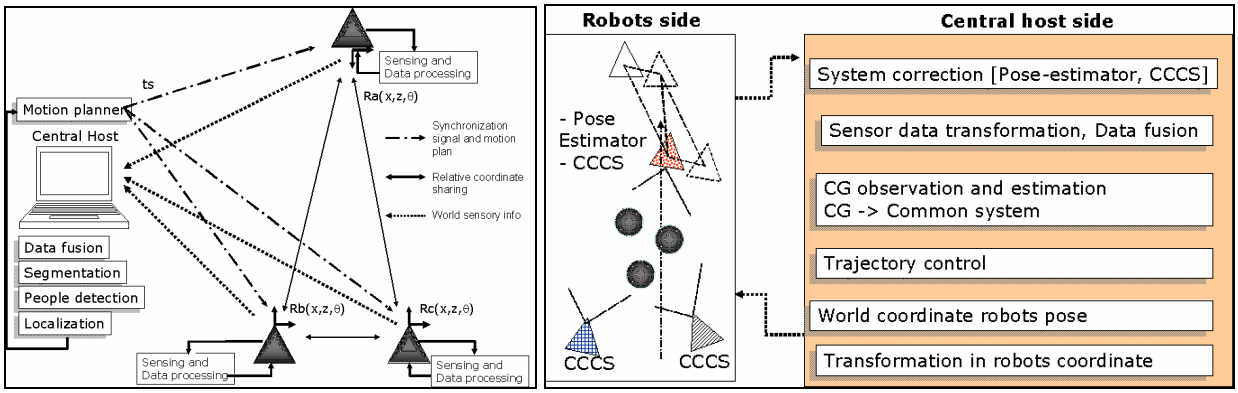

Figure 4. (a) MRS architecture; (b) robots' relative Cartesian system and world representation in the central host

4. Multiple People Localization

In this section, the methodology for multi-human localization is discussed in detail, theoretical foundation and experimental results are shown. Firstly, a team of mobile robots was deployed to localize all the humans in a target-group. A team of robots overcome in great extent the problem of partial occlusion generated by the members themselves. In Fig. 5, the configuration of an experiment is depicted; Basically, for the purpose of evaluation the environment was set a priori within 2 rows of people, 3 and 2 people at front and back respectively, between Ra (front) and Rb, Rc (left, right also respectively).

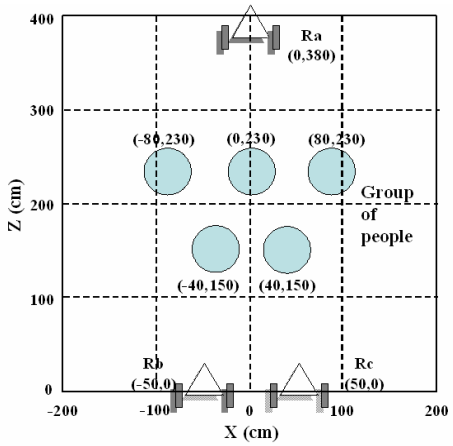

Figure 5. Experiment configuration with 5 people, and 3 mobile robots

From this experimental configuration, the Fig.6 depicts gray level images arising from each robot (from one stereo camera). Actually they do provide their fields of view, at their given geometrical positions, which can be matched with the robots' position at depiction of Fig.6.

Figure 6. Image views from a) Rb, b) Ra and c) Rc

In Fig. 6, from any given location, humans are difficult to perceive totally due to multi-human occlusion. In the case of Ra (Fig. 6-b), it can only sense partial regions from people at the back, and Rb and Rc barely perceive 3 or 4 persons. From the stereo images a ranged world model was obtained, and sensor data (3D) have been plotted in Fig. 7. It shows the sensor readings top view for each of the 3 robots. All plots have been arranged into a common coordinate system.

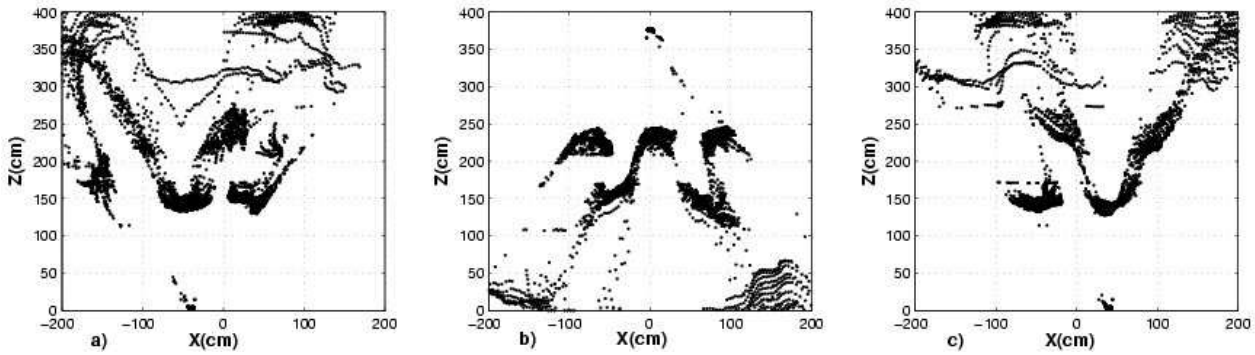

Figure 7. Sensors reading top view, a) Rb, b) Ra and c) RC

As depicted in Fig. 7, due to noise generation, there is uncertainty in sensor data representing the humans.

4.1 Data Processing

A methodology for sensor data filtering, and human localization have been developed, mainly organized by 5 general stages:

1.) Environment sensing (previously introduced)
2.) Filtering:
    a) Zones discrimination
    b) Noise reduction
    c) Quantization filtering
3.) Distributed multi-sensor data fusion
4.) Clustering based segmentation
5.) People localization

Data filtering is considered as an essential part as a preamble for multi-sensor data fusion and people segmentation process. Filtering essentially, is compounded by 3 main parts: 2-(a) zones discrimination, 2-(b) noise reduction and 2-(c) a routine of data quantization working as a spatial filtering. In multi-sensor data fusion (3), the information is arranged onto a common coordinate system to construct a short-term world model. In addition, we have implemented a segmentation method relaying on a clustering algorithm (4). Eventually, people are detected and localized (5).

4.2 Zones Discrimination

A first important regarding in the present strategy for filtering involves a spatial modality, which deals with an early elimination of unnecessary spaces. It has been called zones discrimination process because filtering relays on 2 thresholds. Both thresholds exhibit a couple of heights of the human body (shoulders and keens). Discrimination is applied to points falling out such thresholds; meanwhile, points between them (20 and 40 cm) are considered information with high likelihood to be within the set of points of ranged

people. In general, it was assumed about 170cm as a statistical average for people's height. Let us consider a set called RAW of vectors raw^i, such that RAW={raw^1, raw^2,..,raw^n}, and each vector $raw^i \in \Re^3$, thus raw^i ={raw^i_x, raw^i_y,..,raw^i_z} corresponding to the 3 spatial components. Likewise, let's establish that V is a subset, such that $V \subset RAW$. Thus, our model for point discrimination is expressed in by V={raw^i / th_1<=raw^j<=th_2}. Where, the set RAW represents the raw sensor data, V is the set with the points of interest evaluated by raw^j_y. The range is delimited by $th_{1,2}$ representing knees and shoulders, and points which were ranged out are floor, ceiling and even mismatched points are zones from which sensor generates a considerable large amount of points, and are not useful for our purpose. It can be noticed the difference of quantity and points remaining after the discrimination process. By preserving the points between shoulders and knees, their quantity was approximately 15% of the total being still useful for later processing, while about 85% was removed (see results in Fig.8).

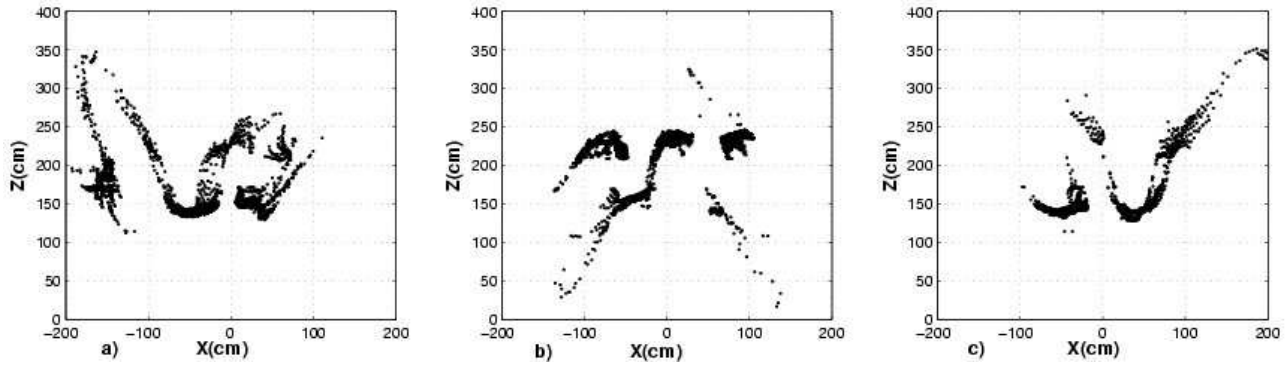

Figure 8. Top view, results of point discrimination, a) Rb, b) Ra, and c) Rc

4.3 Noise Reduction

Noise reduction is an essential task to avoid undesired nosy regions, and keeping a suitable world model, as sensory data is not a perfect noiseless data model. It was implemented a noise reduction spatial filtering for dealing with noisy areas defined as small 3D spaces containing poor density and low uniformity distribution of sensor data, which were about less than 15 3D-points in a volume of 10x10x120cm (XZY) for one robot. Humans on the other side keep a high density and a uniform distribution of points. A suitable solution to tackle this problem was by implementing a 3D spatial filtering window with a threshold of point's number. The filtering window slides over X and Z directions over the ground plane. The filtering discriminates sets of points if their number in the cell, is lower than the threshold. This process is represented by the set $V=\{v^1,v^2,...,v^m\}$. Thus, defining the space $D=\{D^1, D^2,..,D^p\}$, from where each subspace is defined by $D^k=\{d^j_1,d^j_2,..,d^j_l\}$ containing a number l of points $(dj^i)^l_{i=1}$ to be evaluated in expression (1), the filtering-window in process state is called the j^{th} cell, such that its upper left coordinates are given by (x_j,z_j) and size by *fwin*. Thus, results are then evaluated by (2) into the set H. Regarding a number of points called l and restricted by a threshold th_n, the action of filtering is given by (3),

$$D^j = \left\{ v^i \mid x_j \le v^i_x \le x_{j+fwin} \wedge z_j \le v^i_z \le z_{j+fwin} \right\} \quad (1)$$

$$H^k = \begin{cases} D^j, & l \ge th_n \\ \phi, & other \end{cases} \quad (2)$$

Where $H \subset V$, such that $H=\{H^1,H^2,..,H^p\}$ and $H^j=\{h_j^1,h_j^2,..,h_j^l\}$ for $hj^i \in \Re^3$. Likewise, the filtering area was given by fwin=10cm and threshold equal to 20 points for the present experiments. The results from each robot are plotted in figure 9-a), b), c). With this algorithm in all experiments, data were still reduced about 27% less (from the resulted after zones discrimination), remaining approximately 73% for latter processing (although it was depending on the cell size).

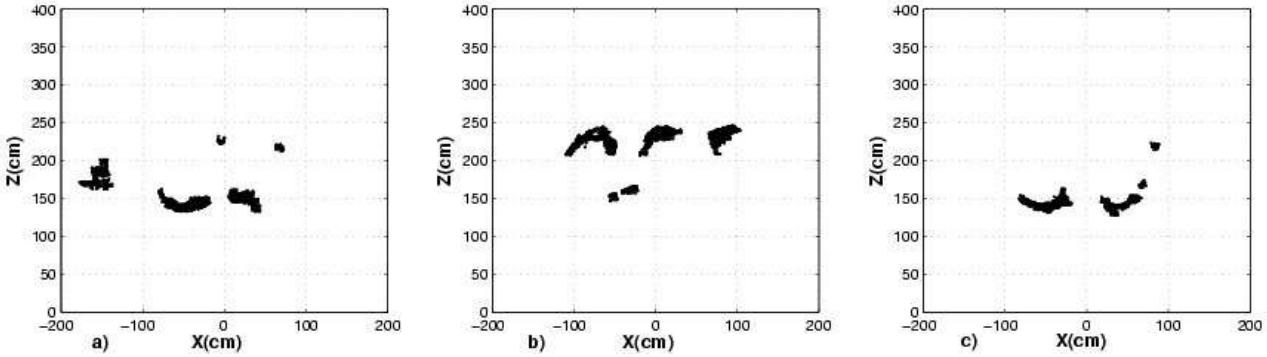

Figure 9. Results of noise reduction process. a) Rb, b) Ra and c) Rc

The people who were partially or completely occluded by other people hardly might appear in the sensory model after noise reduction, due to poor density of points.

4.4 Quantization Filtering

The purpose of quantization is a reduction of points that decreases considerably more the burden of computation, and projects 3D points into a 2D model, as the latter is enough to represent humans' position. Moreover, this task aims to project objects' within a lower density of points. The principle of this algorithm is a quantization of points in the XZ space, performing a filtering through a small square cell. Regardless the number of points within the cell, if it keeps at least one point, then only the central value of the actual cell will represent such cell-area. It was found that it did not affect the final occupancy data representation on the XZ space, because of the small size of the cell. Thus, our model is given by two sets of vectors in $\Re^3$, where H is the set of vectors of the filtered data from (3), and C is a new set, which its space XZ is divided by a new size of cells represented by hwin. Where $C=\{C^1, C^2,..,C^q\}$ and $C^k=\{k, k,..,k\}$, and C^k contains the k^{th} cell index as many times as the number of points in such cell. For points reduction, XZ space will be split and referenced by cell addresses as expression (3), whereby h^i_x is transformed by $((h^i_x)/(hwin)+1)>0 \ \forall \boldsymbol{Z}$ being Z the set of integers. Then transforming the space H into a C space,

$$C^k = \left\{ k \,|\, \left(\frac{h_x^i}{hwin} \right) + 1 = x_k \wedge \left(\frac{h_z^i}{hwin} + 1 \right) = z_k \right\} \tag{3}$$

Thus, the set of points in each cell are defined in the domain of the set C^k, additionally let's define the center of the cell H^k by $(x_k+hwin/2)$ and $(z_k+hwin/2)$, where every cell origin is given by (a_k,b_k) in cm. In Fig. 11-b), each cell has a determined number of points, and those points are labeled or referenced with their respective number of cell given by (3). The sense of this technique is for representing the content of a cell, instead of considering all the points in it, as in Fig. 11-c). From here, as depicted in Fig. 11-d), only one 2D point is considered, and it will appear at every non-empty cell.

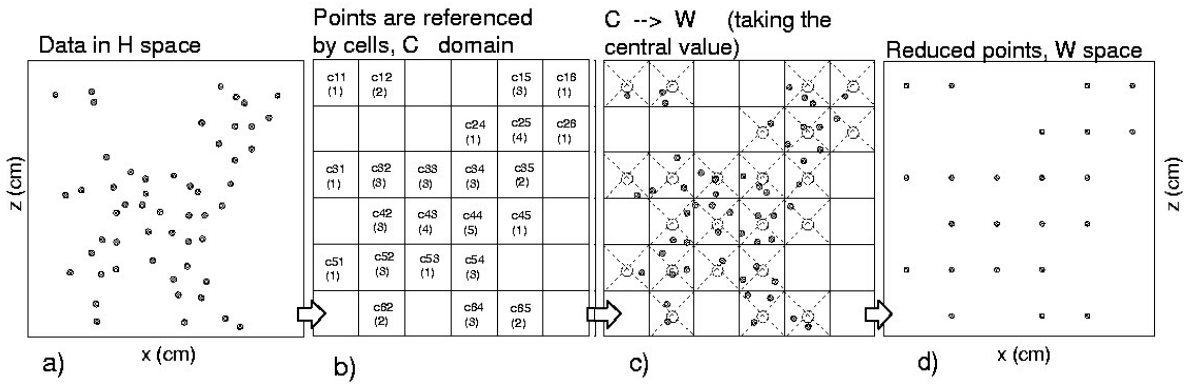

Figure 10. Point reduction process

Eventually, the process of data reduction is calculated, resulting the set $W=\{W^1,W^2,..,W^q\}$. The mechanism of point reduction was by the expression (4) which not only converts cell dimension data into the original XZ-space points, but also calculates the central cell-value.

$$W^k = \begin{cases} \phi, & C^k = \phi \\ (x_k + \dfrac{hwin}{2}, z_k + \dfrac{hwin}{2}), & otherwise \end{cases} \tag{4}$$

The space is basically a grid where each unique cell contains a different number of xz-points, such that by considering the C space it resulted more suitable to compute small number of cells with points having a same label, than a large number of points addressed by an XZ coordinate (H domain), see figure 10-a). In general, the rate of 2D points was highly reduced as well as time computation for latter data processing. Its significance comes from the fact that once data fusion is performed the total number of points (from the team of robots) will generate a certain huge burden for segmentation performance. Results of point quantization are depicted in Fig. 11.

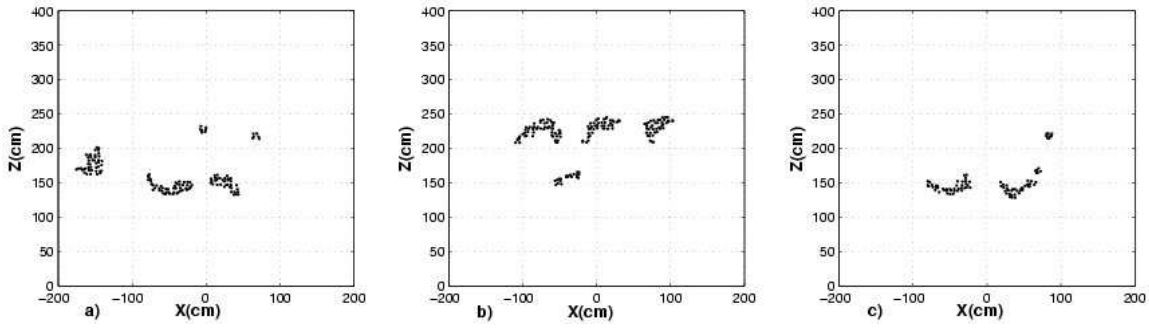

Figure 11. Point reduction results, robots a) Rb, b) Ra and c) Rc

The number of 3D points was reduced over 15,000 from the original ones (raw data) only in Ra. Practically, by means of this process nearly 93% of the data was still removed without lose 2D occupancy of ranged objects (people and furniture). Thus, for the purpose of data fusion about 7% of the points in each robot have resulted. Now on, these results can be more advantageous, and segmentation can be more likely attained.

4.5 Data Fusion, Segmentation and People Localization

The aim of multi-sensor fusion in the proposed method is to yield a global model of the world by sharing local sensory data arising from each robot's location. The way of data

association is by setting onto a common coordinate system the sensory information filtered by each robot. Multi-sensor data fusion makes possible to reconstruct objects that do not exist in the data model of a determined robot's sensory info. In addition, a sensor-sensor calibration was required for attaining accurate data fusion. To overcome the problem of dynamic distributed sensor data calibration, 4 main parts (among other very particular details) were implemented in the architecture:

1.) Multi-robot positions (attained by the CCCS).
2.) Sensor data calibration (correction of Cartesian errors in sensors fixation).
3.) Synchronized sensing. (same spatial-temporal sensor data is fused).
4.) Transformation of sensor data (for representation in a common world coordinates).

Once data fusion process has been carried out, clustering based segmentation is then performed as a preamble to typify the nature of the objects. Multi-sensor data fusion is carried out in the central host at every discrete time t_k. Further than improve the state of a world model at every updating, it has only a short-term purpose and its time of life is limited to less than the updating time. Thus, the points in $w^i=(w^i_x, w^i_y, w^i_z)$ were translated by (5) according to their positions (x_r, z_r) and heading angles θ_R by,

$$\begin{pmatrix} \omega^i_x \\ \omega^i_z \end{pmatrix} = \begin{pmatrix} Cos(r_\theta) & -Sin(r_\theta) \\ Sin(r_\theta) & Cos(r_\theta) \end{pmatrix} \begin{pmatrix} w^i_x \\ w^i_z \end{pmatrix} + \begin{pmatrix} r_x \\ r_z \end{pmatrix} \tag{5}$$

Global coordinates were computed in (ω^i_x, ω^i_z) as a previous step for data fusion process. Now on, the set K holds a model representation of the environment which is the result of data fusion given by the following expression $K=[\omega]_a \cup [\omega]_b \cup [\omega]_c$. Finally, such expression determines the space K which represents the short-term world model (see results in Fig.12-(a)). This data model is now a key-issue for the process detailed in next section.

How to determine what set of points are representing a unique object was established by grouping 2D points which their unique common feature is a distance that differentiates what group of near points belongs to a particular object. The purpose of any clustering technique is to evolve a K x r partition matrix of data set $S(S=s^1,s^2,..,s^r)$ in $\Re^N$, representing its partitioning into a number of sub-clusters, say k, of clusters (Bandyopadhyay & Maulik, 2000). The method for segmentation is based upon a threshold distance between two points in the set K. If two points are close enough, then those given points are labeled as part of a same subgroup. A determined point in process of clustering is compared with the rest in the total set.

The end of such process ends up with a group of clusters representing the objects in the area surrounded by the team of robots. The method presented in this context has three main bases as core for segmenting:

1. Unclassified point vs. unclassified point

When 2 points $p=(p_x,p_y,p_z)$ and $q=(q_x,q_y,q_z)$ have not been labeled yet, and are close enough that an distance d between them is shorter than the established threshold d_{th} ($d \leq d_{th}$), then both points are classified as part of the same sub-cluster S^1, represented in expression (6) as,

$$\sqrt[2]{(px-qx)^2+(pz-qz)^2} \leq d_{th} \Rightarrow S^1 = \vec{p} \cup \vec{q} \tag{6}$$

2. Unclassified point vs. classified point

When a point $p \in \Re^3$, which is non-classified yet and is close enough to the point s^i in sub-cluster S^1 that the distance between them is such that $d \leq d_{th}$, then set and point will be classified as part of the same sub-cluster, in S^2 represented by the subset of the equation (7).

$$S^1 \neq \phi, \sqrt[2]{(p_x - s^{1i}_x)^2 + (p_z - s^{1i}_z)^2} \leq d_{th} \Rightarrow S^2 = \vec{p} \cup S^1 \tag{7}$$

3. Classified point vs. classified point

When 2 sub-clusters of points S^1 and S^2, which are already pre-classified and are close enough that at least a point of both groups (S^1 and S^2) are close enough that $d \leq d_{th}$, then set S^1 and set S^2 will be classified as part of the same sub-cluster, in S^3 represented by the subset of the equation (8).

$$S^1, S^2 \neq \phi, \sqrt[2]{(s^{1i}_x - s^{2j}_x)^2 + (s^{1i}_z - s^{2j}_z)^2} \Rightarrow S^3 = S^1 \cup S^2 \tag{8}$$

In situations like the previously explained once the points has been totally labeled, the set K is partitioned in r^{th} subgroups of vectors called $S^k=\{s^{k1}, s^{k2},..,s^{kr}\}$, where each of such points has in common a label value. Now let's say that the distance threshold was denoted by $d_{th}=15cm$. Segmented objects are classified by a determined numeric label generated and assigned automatically during the process as depicted in Fig.12-(b).

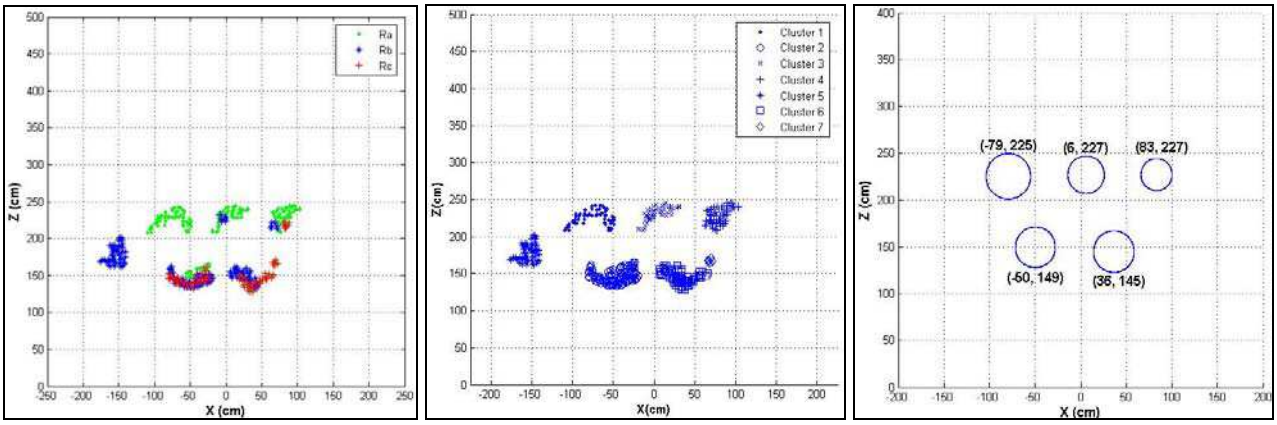

(a) (b) (c)

Figure 12. (a) Multi-sensor data fusion; (b) segmentation results; and (c) multi-people localization results

In Fig. 12-(b), only 6 clusters of points were found by performing the algorithm. Noting that clusters 5th and cluster 7th, the former one represents a section of a furniture, which at the time of the experiment it was in the field of view of *Rb*. Likewise, cluster 7th, is a small fragment of bit of noise associated with a part of data people. In spite of that, cluster 7th is considered as noise because in any possible manner it does not have enough size-feature as humans, such as the number of points, height, width and depth. A similar consideration was taken for the cluster 5th, because it is not as tall enough as a human. Basically size constraints were established a priori to differentiate humans from other objects, for this process we regarded some parameters such as clusters' center of gravity (x,z), number of points, maximum and minimum values of the XZ-space as height of each object. Fig. 12-(c) shows how humans have been successfully localized; each circle expresses humans' positions. Their scopes surround the highest concentration of ranged points close to their

center of gravity. Basically human's positions were represented by their center of gravity. For depiction of humans' scope the clusters' standard deviation σ_d was deployed as radius d for drawing the circles. For the subfigure 12-(c), circles were plotted with radius of $3\sigma_d$. Similar works with distributed networked systems for multi-people tracking but different contexts were presented by (Nakazawa et al., 1998; Tsutsui et al., 2001).

5. Strategy for People Trajectory Control

Localizing every human in a group is an approach that allows an estimation of the people group's center of gravity (CG). In such estimation, a noisy computation of CG is regarded for several causes such as missing the measurement of a human due to temporal members' occlusion, or bad light conditions and so forth. A strategy for improving the observation of the CG is a critical issue to yield trajectory control. A proposed framework for controlling the trajectory of the group's CG is presented in Fig.13.

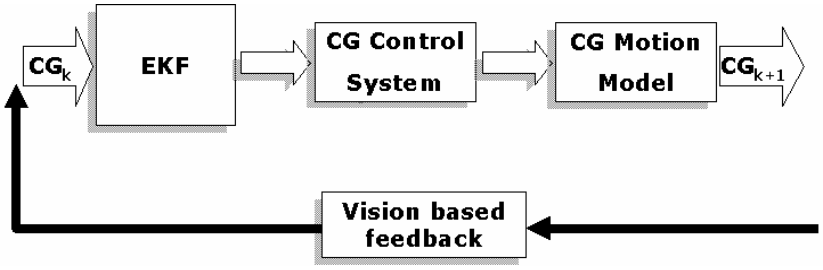

Figure 13. Block diagram of the vision-based feedback control

The CG observation is easily accomplished by calculating it after multi-people localization. CG estimation is a filtered version of the CG carried out by a traditional extended Kalman filter. The trajectory control system provides a way for steering the CG leading to track a desired pathway. Eventually a motion model allows predicting into discrete time k+1 a desired CG position.

5.1 Trajectory Control Model

A principle in the proposed method is that the team of robots must steer the GC towards a desired pathway. The equation (10) expresses a model of the CG angular acceleration (α_k), it yields a trajectory tracking while moving from the actual GC location towards the tracking-line having a distance Δx between to be reached. Nevertheless, the robots team can not explicitly control such α_k, but can in some extent affect the CG heading angle θ at navigation time. The equation also requires the CG's angular velocity wk feed at every cycle. In this context the equation (9) models a lineal feedback control.

$$\alpha_k = -k_1 \Delta x_k - k_2 \theta_k - k_3 w_k \tag{9}$$

The gain is established by the constants k_1, k_2 and k_3 and were determined by trial and error for the robots. The steps for calculating a desired CG's location at time k+1 is by correlating the previous equation value α_k with the set of equations that model the kinematics of motion of the CG (not the control). The fig.14-(a) shows a depiction of the kinematical parameters regarded for its control already discussed. CG is a dynamic particle surrounded by a circular scope, which is defined by the magnitude of the crowding (members of the group). For its control every member's dynamic status is

averaged in its CG's behavior.

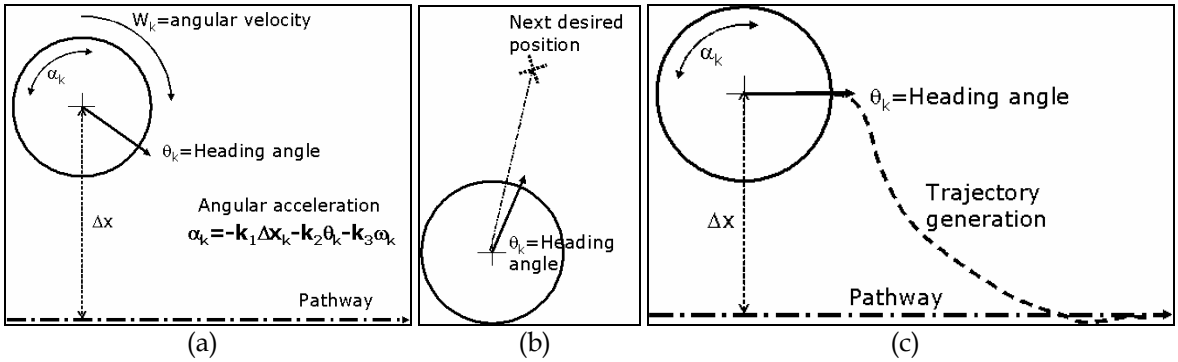

Figure 14 (a) Feed-back control model; (b) Motion model; and (c) Control and trajectory generation

5.2 Group's Motion Model

As depicted in Fig.14-(b) regardless the actual kinematical tendency at time k of the CG, there exist need to determine a desired future position value at k+1 to properly yield control over x and z coordinates for the CG's trajectory. A proposed motion model for the CG correlates a set of simple equations for getting regarding a new pose Pk+1 at certain desired velocity. A projection of the group's angular velocity wk+1 is given by the equation (10), involving a measurement of the actual w_k and α_k. The result from equation (10) allows to correlate a prediction of the current angle θ_k into next discrete time θ_{k+1} by (11) as

$$w_{k+1} = w_k + \alpha_k \Delta t \tag{10}$$

$$\theta_{k+1} = \theta_k + w_{k+1} \Delta t \tag{11}$$

Basically, the previous scalar results become fundamental to obtain lineal results in velocity and distance of the CG as vector representations yielded by expressions (12) and (13).

They exhibit a more representative condition of the CG's motion behavior. Certainly, lineal velocity and distance vectors in $\mathcal{R}^2$ (x, z components). Being γ the gain that provides a control behavior to the vector velocity $\boldsymbol{v}$ on how fast it is stabilized in (12). A desired velocity v_{ref} is a constant value established a priori. Eventually, the model for predicting a next desired position of the CG is yielded by equation (13) as,

$$\vec{v}^{\,x}_{k+1} = \vec{v}_k + \gamma \ (v_{ref} - \vec{v}_k) \tag{12}$$

$$\vec{P}_{k+1} = \vec{P}^{\,x}_k + \vec{v}_{k+1} \Delta t \tag{13}$$

Thus, angular velocity, heading angle, velocity and position vectors are the variables that define the proposed CG motion model. In fact the group of people kinematics is seen and analyzed throughout its CG considered as a self-driven particle.

The Fig.15 shows the results obtained by merging the control and the motion model for the CG. In the simulation the CG started at 100 cm away from the tracking line heading towards 60° with a sequence of Gaussian noise a long with the trajectory generation data. The sampling time was established in 0.125 sg, CG displacement over time was vx=0.1m/sg, vz=0.5m/s and angular velocity w_k=10°/s. Likewise for this simulation results k_1=3.66, k_2=2.5 and k_3=-7.54. Besides in the plotting the angle control, x-velocity and z-velocity behaviors are depicted.

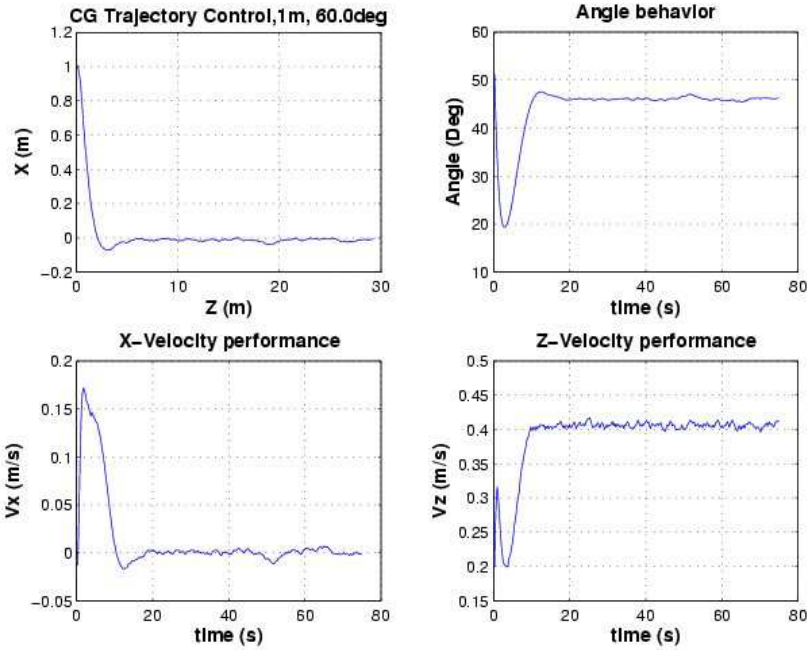

Figure 15. Results of the trajectory control merged with the motion model results

5.3 Center of Gravity Estimation

One of the major important issues for the mechanism to control the CG is the measurement of it, which yields noisy observations. A proposed solution is the implementation of a traditional version of the Extended Kalman Filter (EKF) (Kalman, 1996 ;Meybeck, 1979; Welch & Bishop, 2002) that resulted to be suitable enough to overcome the problem of noise filtering and to get present and future estimations of the CG kinematics. The state n-vector of the process $\mathbf{x}_k = (x, z, \theta, v, w)$ at discrete time k defines the group's pose (x,z), lineal and angular velocities *v*,*w* respectively. The observation of the system, which relates the sensory information is expressed in $\mathbf{z}_k=(x;z)$ as in equation (14) and Kalman gain K in (15).

$$\vec{z}_k = H\vec{x}_k + \vec{u}_k \tag{14}$$

$$K_k = P_k H^T (HP_k H^T + R_k)^{-1} \tag{15}$$

Likewise, the present implementation also included the variable $H_{[2x5]}$ stationary over time matrix noiseless connection between the vectors $\boldsymbol{x}_k$ and $\boldsymbol{z}_k$, and the $\boldsymbol{u}_k$ that correlated a Gaussian white sequence.

$$\bar{x}_k = \hat{x}_k + K_k(\vec{z}_k - H\hat{x}_k) \tag{16}$$

$$\hat{P}_k = P_k - K_k HP_k \tag{17}$$

It was possible to write an update equation for the new estimate $\mathbf{x}_{k+1}$, combining the old estimate $\mathbf{x}_k$ with the measurement data $\mathbf{z}_k$. Additionally, a subsequent part of estimation process suggests also the update covariance matrix over time. Basically, the projection of estimate $\mathbf{x}_{k+1}$ and the vector state error covariance matrix.

$$\bar{x}_{k+1} = \Phi\hat{x}_k + q_k \tag{18}$$

$$\bar{P}_{k+1} = \hat{P}_k + (A + A^T)\hat{P}_k\Delta t + (A\hat{P}_k A^T + \Sigma_w)\Delta t^2 \tag{19}$$

Also the EKF equations express the projection into k+1 of previous estimate $\mathbf{x}_k$, and it relates the state transition matrix of the process $\boldsymbol{\Phi}$ (also non-stationary), and projection into k+1 of the covariance is involved. Fig.16 depicts the results obtained from merging the EKF with the trajectory control and motion models.

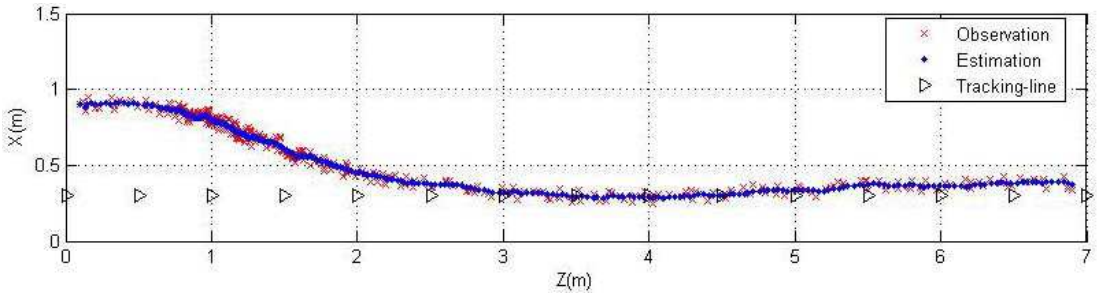

Figure 16. Kalman filter with trajectory control simulating cg's behavior

The observations of the CG are symbolized by a cross character, at less than 90 cm away from the tracking-line heading 10° (observations include Gaussian noise), and sampling time was set to 0.10 sg for 350 discrete samples and an angular velocity *w*=10°/sg.

7. Robots Motion Planning

The basic principle relays on the fact that a single robot (Ra) is suitable enough to provide guidance (not control). Meanwhile the rest of the robots at back are purposed to share observations and controlling the size of the people dispersion. Figure 17-(a) depicts a circular model encompassing the group and its model for to determine a desired size r_{k+1} is given by the expression (20). The main element for affecting the crowd dynamics relays on changing the actual radius r_k until reaching a desired radius r_{ref} (established a priori) by deploying the robots at certain positions and speeds. If the condition r_k is $r_k > r_{ref}$ exists, the process of crowding is performed (the smaller the r_k, the more the crowding). In this strategy the team of robots gets closer or farther from the CG, forcing the people to modify their inter-space. Once the trajectory control yields the next desired CG, the radius is measured and a robots motion plan takes is performed

$$r_{k+1} = \begin{cases} r_k + \beta(r_{ref} - r_k), & r_k > r_{ref} \\ r_{ref}, & r_k \le r_{ref} \end{cases} \tag{20}$$

The *Ri* (i={a,b,c}) poses are determined based on the CG location as depicted in Fig.17-(b), according to the angles given by δ_i. Δs is the distance required for the field of view of the sensors settled as a constant. Moreover, the heading angle for the team of robots is already given by the Kalman filter equations leading towards the desired pathway.

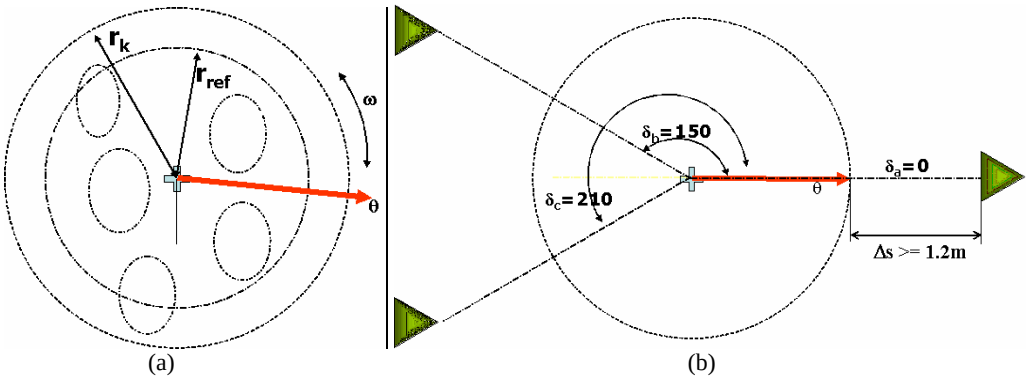

Figure 17. (a) Group's size control model and parameters; (b) configuration of robots' formation

Since the team of robot must reach certain position at k+1 for yielding control of the group's size, the change of speeds are given by the equation (21), where Ri is the vector pose of robot i at every discrete time interval Δt.

$$V_{k+1} = \frac{\left| Ri_{k+1} - Ri_{k+1} \right|}{\Delta t} \tag{21}$$

7. Simulation of People Group under Trajectory Control

In reference (Kirkland & Maciejewski, 2003), an attempt to simulate crowd dynamics by pedestrians affected by the presence and introduction of mobile robots was presented. Such context considers a large number of pedestrians and few robots in order to study and understand its impact and effect in wide areas people behavior. That reference as the present work is considering the usage of the Social Force Model (SFM) originally introduced by (Helbing & Molnar, 1995). However, in the present work, the model proposed by Helbing has a different application as we attempt to adapt the model to simulate a reduced number of pedestrian behaving as a group following the leader robot Ra and affected by the presence of robots Rb and Rc. It is suggested that the motion of pedestrians can be described as if they would be subject to social forces. The corresponding SFM can be applied to several behaviors. It describes the acceleration towards a desired velocity of motion; it also terms reflecting that a pedestrian keeps a certain distance from other pedestrians and borders; and a term modeling attractive effects. The equations of the SFM involve: (1) A model for the desired direction of each pedestrian; (2) models repulsive effects (avoid obstacles and/or other member of the group); (3) models attractive effects (pursuing Ra, a chatting with other members); and (4) models some random variations of the behavior. Until this stage we have obtained experimental results in laboratory with the team of robots and sensors data. However, a simulation model can give us good approaches to prove the effectiveness of the proposed trajectory control model, and the verification of the methodology and strategy. Moreover simulation let us confirmation of the proposed people trajectory control with the robots motion planning. Finally, a human motion modeling can be generated. The algorithm that was implemented for simulation is described as following:

1) An initially random location of the members.
2) Members pursuit to Ra's orthogonal line respect to Ra's heading angle.
3) The CG observation and group size (rk) is provided.
4) Estimation of the CG (filtering) is yielded.
5) With the CG estimation a next desired (controlled) position is obtained by merging of the trajectory control and CG motion model.
6) The next desired radius is determined (the farthest member is the actual maximum radius).
7) Robots move towards their angles depending on CG's position and heading.
8) Again from step 2).

With this algorithm, figure 11 depicts the simulation results for the conduction task, by merging all the models proposed in this paper.

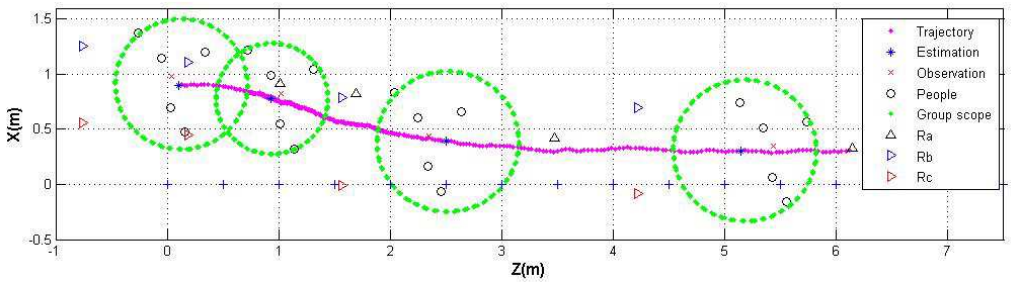

Figure 18. Simulation results of the guiding-task. Merging of the Kalman filtering, the CG-trajectory control model, the CG-prediction motion model and the robots motion plan

8. Conclusions and Future Work

It has been considered that an important issue of this research work relies on the regarding of this modality for people conduction. A given contribution has been the methodology for conduction, its strategy for accomplishing the task-goal and the implementation of the system itself. It has been considered that most important issues featuring the present architecture are synthesized as:

1.) A framework for people trajectory control model.
2.) Guidance is mainly constrained by being of implicit communication type.
3.) Motions reactions are the means of interaction for trajectory control between robots and people.
4.) Non-active cooperation modality is given by the robots in this architecture.

Furthermore, there are some important points of the guiding situation style, which were regarded as the basis for the MRS architecture. Likewise, some of the functionalities and part of the strategy for accomplishing conduction tasks that still deserve further considerations for investigation. For mentioning some of them; while conduction, people's assumptions are tied to the fact that they follow Ra, and/or just follow the crowd towards Ra's direction (specifying that direction for navigation is determined by Ra). The philosophy for attaining conduction is leader-based robots' formation, and several robots surround the group of people (it does not happened in other related work). Part of what affect psychologically the target-group people during the conduction task is that they walk feeling of being observed and the approach of back's robots. The team of robots affects the group's crowd dynamics depending on positions and speeds. Besides, summing up in the scope of this work a multi-robot system architecture purposed to guide a group of people, a vision-based multi-people tracking by team of robots, a trajectory control model and a robots motion planning system were discussed. In the present context the approach has been to depict results of successful multiple people localization. We discussed in detail a method by deploying a MRS within a centralized architecture, since it has resulted enough for a task-oriented approach. The content of this paper is a critical part as a preamble to accomplish real experiments for interaction with different social groups of people aimed to provide guiding-tours. A methodology for processing and sharing distributed sensor data and multi-sensor data fusion was detailed with experimental results by deploying a team of 3 mobile robots, as well as evaluating robustness and reliability of the methods.

9. References

Bandyopadhyay S. & Maulik U. (2000). Performance evaluation of some clustering algorithms and validity indices, IEEE Tran. on Pattern Analysis and Machine Intelligence, 12, 1650-1654.

Beymer D. & Konolige K. (1999). Real-time tracking of multiple people using continuous detection. In Proceedings of IEEE International Conference on Computer Vision.

Burgard W., Cremers A., Fox D., Haehnel D., Lakemeyer G., Schulz D., Steiner W., & Thrun S., (1999) Experiences with an Interactive Museum Tour-Guide Robot, Journal of Artificial Intelligence, Vol. 114, No. 1-2, pp. 3-55.

Cao Y., Fukunaga A. & Kahng A., (1997) Cooperative mobile robotics: Antecedents and directions. Autonomous Robots, 1, 2-27.

Helbing D. & Molnar P., (1995) Social force model for pedestrian dynamics. Physical Review E, Vol. 51, No. 5, pp. 4282-4286.

Iocchi L., Nardi D., Piaggio M. & Sgorbissa A. (2003) A Distributed Coordination in

Heterogeneous Multi-Robot Systems. Autonomous Robots, 5, 155-168.
Kalman R., (1996) A New Approach to Linear filtering and Prediction Problems. Transaction on the ASME-journal of Basic Engineering, 82 (Series D), pp. 35-45.
Kirkland J. and Maciejewski A., (2003) A Simulation of Attempts to Influence Crowd Dynamics. IEEE Int. Conference on Systems, Man, and Cybernetics, pp. 4328-4333, Washington, DC, 5-6.
Martinez E., Ohya A., Yuta S., (2003) Recognition of people's positioning by multiple mobile robots for humans groups steering, In Proceedings of Computational Intelligence in Robotics and Automation, Kobe Japan, pp. 758-763, 2003.ISBN 0-7803-7866-0/03.
Martinez-Garcia E,, A., Ohya & S., Yuta, (2004) Multi-people Localization in by Multiple Mobile Robots: First Approach for Guiding a Group of Humans, International Journal of Advanced Robotics Systems, Vol.1, No.3, pp.171-182.
Martinez-Garcia E., Ohya A. & Yuta S., (2005) A multi-robot system architecture communication for human-guiding, to appear in the Journal of Engineering Manufacture Part B1, Vol.256, January.
Maybeck P., (1979) Stochastic models, estimation, and control. Vol. 1, Academic Press, Inc. LTD.
Murphy R., (2000) Introduction to AI Robotics, The MIT Press, ISBN 0-262-13383-0, Massachusetts Institute of Technology.
Nakazawa A., Kato H. & Inokuchi S. (1998). Human tracking using distributed vision systems. 14th International Conference on pattern recognition, pp. 593-596, Brisbane, Australia.
Nourbakhsh I., Bobenageb J. & Grangec S., Ron Lutzd, Roland Meyerc and Alvaro Sotoa, (1999) An Affective Mobile Robot Educator with a Full-time Job, Artificial Intelligence, Vol. 114, No. 1-2, October, pp.95-124.
Thrapp R., Westbrook C. & Subramanian D., (2001) Robust localization algorithms for an autonomous campus tour guide, In Proceedings of International Conference on Robotics and Automation, Vol. 2, pp. 2065- 2071.
Tsutsui H., Miura J. & Shirai Y. (2001). Optical flow-based person tracking by multiple cameras., In Proceedings of IEEE Int. Conf. On Multisensor Fusion and Integration in Intelligent Systems, Baden-Baden, Germany.
Watanabe Y. & Yuta S.,(1990). Position estimation of mobile robots with internal and external sensors using uncertainty evolution technique. In proceedings of IEEE Int. Conf. Robotics and Automation., Cincinnati, OH., pp. 2011-2016.
Welch G. & Bishop G., (2002) An Introduction to the Kalman Filter. UNCChapel Hill, TR 95-041.
Yoshida T., Ohya A. & Yuta S., (2003). Cooperative self-positioning system for multiple mobile robots. In Proceedings of IEEE International Conference on Advanced Intelligent Mechatronics, pp. 223-227.

Cutting Edge Robotics

Edited by Vedran Kordic, Aleksandar Lazinica and Munir Merdan

ISBN 3-86611-038-3

Hard cover, 784 pages

Publisher Pro Literatur Verlag, Germany

Published online 01, July, 2005

Published in print edition July, 2005

This book is the result of inspirations and contributions from many researchers worldwide. It presents a collection of wide range research results of robotics scientific community. Various aspects of current research in robotics area are explored and discussed. The book begins with researches in robot modelling & design, in which different approaches in kinematical, dynamical and other design issues of mobile robots are discussed. Second chapter deals with various sensor systems, but the major part of the chapter is devoted to robotic vision systems. Chapter III is devoted to robot navigation and presents different navigation architectures. The chapter IV is devoted to research on adaptive and learning systems in mobile robots area. The chapter V speaks about different application areas of multi-robot systems. Other emerging field is discussed in chapter VI - the human- robot interaction. Chapter VII gives a great tutorial on legged robot systems and one research overview on design of a humanoid robot.The different examples of service robots are showed in chapter VIII. Chapter IX is oriented to industrial robots, i.e. robot manipulators. Different mechatronic systems oriented on robotics are explored in the last chapter of the book.

InTech Europe
University Campus STeP Ri
Slavka Krautzeka 83/A
51000 Rijeka, Croatia
Phone: +385 (51) 770 447
Fax: +385 (51) 686 166
www.intechopen.com

InTech China
Unit 405, Office Block, Hotel Equatorial Shanghai
No.65, Yan An Road (West), Shanghai, 200040, China
中国上海市延安西路65号上海国际贵都大饭店办公楼405单元
Phone: +86-21-62489820
Fax: +86-21-62489821